Program Digest, 2019 IEEE International Ultrasonics Symposium (IUS)
Glasgow, Scotland, October 6-9, 2019

Extension of Coherent Multi-Transducer Ultrasound Imaging with Diverging Waves

1st Laura Peralta
Dept. of Biomedical Engineering
School of Biomedical Engineering & Imaging Sciences
King's College London, London, UK
laura.peralta_pereira@kcl.ac.uk

2nd Michael Reinwald
Dept. of Biomedical Engineering
School of Biomedical Engineering & Imaging Sciences
King's College London, London, UK
michael.reinwald@kcl.ac.uk

3rd Alessandro Ramalli
Dept. of Cardiovascular Sciences
KU Leuven, 3000 Leuven, Belgium
alessandro.ramalli@unifi.it

4th Joseph V Hajnal
Dept. of Biomedical Engineering
School of Biomedical Engineering & Imaging Sciences
King's College London, London, UK
jo.hajnal@kcl.ac.uk

5th Robert J Eckersley
Dept. of Biomedical Engineering
School of Biomedical Engineering & Imaging Sciences
King's College London, London, UK
robert.eckersley@kcl.ac.uk

***Abstract*—The assessment of ultrasound images is hampered by limited spatial resolution and view-dependent artifacts. Both limitations depend on the small aperture of the transducers used in clinical practice, and may potentially be overcome by extending the effective aperture. The coherent multi-transducer ultrasound (CoMTUS) imaging method enables an extended effective aperture through coherent combination of multiple transducers. In this work, CoMTUS, originally developed and validated using plane waves, is extended to diverging wave imaging to widen the field of view, which, in CoMTUS, is limited to the intersection of the combined field of views. First phantom images produced using CoMTUS with diverging waves are presented here. Results show that CoMTUS with diverging waves has the potential to improve ultrasound image quality, improving resolution and target detectability. Compared with coherent DW compounding using a single probe, there is an averaged improvement in resolution of 26% and 2.3 dB increment in contrast.**

***Index Terms*—Ultrasound Imaging, Diverging Waves, Large Aperture, Beamforming, Image Resolution**

I. Introduction

Limited resolution and a restricted field of view (FoV) are two of the main challenges in ultrasound imaging that, in principle, can only be improved with larger apertures [1]. Recently, we have demonstrated that multiple synchronized arrays, taking turns to transmit plane waves (PWs) into a common FoV, can be used as one large effective aperture to significantly improve imaging resolution [2], [3]. The optimal beamforming parameters, which include the transducer locations and the average speed of sound in the medium, are deduced by maximizing the coherence of the received radio frequency data (RF) by cross-correlation. For this coherent multi-transducer ultrasound (CoMTUS) system an overlap of the isonated regions is mandatory to determine the relative probe-to-probe position [4].

However, for applications that require large and deep FoV, such as transabdominal fetal imaging, a PW approach restricts the applicability of CoMTUS. Like in coherent PW imaging [5], CoMTUS may become rapidly inefficient when the imaging depths are large in comparison with the single apertures, because the different transmitted PWs do not overlap in the region of interest [4]. A solution to the small FoV obtained by PW is the use of circular waves also known as diverging waves (DWs). These waves remain circular during propagation and enable to isonate a large FoV [6]. In this work, we adapt CoMTUS to DW imaging not only to improve resolution but also to extend the width of the imaging FoV.

II. Beamformation

The concept of CoMTUS with DWs is illustrated in Fig. 1. The CoMTUS system considered in this work consists of two identical linear arrays that are synchronized and take turns to transmit a DW. They share part of the FoV and lay on the same plane ($y = 0$). A chosen number of DWs defined by their virtual source (VS) are sent independently by each linear array probe, in an alternating sequence. Each DW is backscattered by the medium and all the transducers that form the system (including the transmitting one) simultaneously receive the corresponding echoes. In a sequence in which transducer i transmits and transducer j receives, the RF data received on channel h of transducer j at time t is named $T_iR_j(h,t)$. The resulting image and all transducer coordinates are defined in a world coordinate system arbitrarily located in space $(\hat{x}_0, \hat{z}_0)$. For each transducer, a local coordinate system $(\hat{x}_i, \hat{z}_i)$ is defined at the center of the transducer surface with the $\hat{z}$ direction orthogonal to the transducer surface and directed away from transducer i. The position and orientation of transducer i are then characterized in the world coordinate system with 3 parameters, a translation vector $\mathbf{r}_i$ and a rotation angle θ_i [7].

Taking into account the full path length between the transmit transducer and the receive elements, a coherent summation is

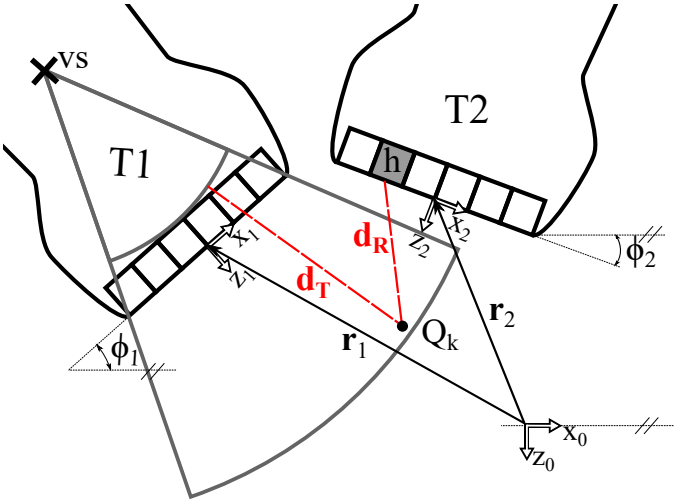

Fig. 1. Multi-transducer beamforming scheme for DWs. In this example, transducer T1 transmits a DW defined by VS and T2 receives the echo scattered from Q_k on element h.

then performed at each point of the image with the adequate delay (Fig. 1). Assuming that transducer i transmits a DW defined by a VS, the image point to be beamformed located at Q_k can be computed from the echoes received at transducer j as:

$$s_{i,j}(Q_k;\mathrm{VS}) = \sum_{h=1}^{H} T_i R_j\,(h, Q_k;\mathrm{VS}) = \sum_{h=1}^{H} T_i R_j\left(h, \frac{D_{i,j,h}(Q_k;\mathrm{VS})}{c}\right) \tag{1}$$

where H is the total number of elements in the array and c is the speed of sound of the medium. The total distance $\mathrm{D}_{i,j,h}(Q_k)$ between the transmit transducer i, the imaging point Q_k and the receive element h of transducer j is defined by,

$$\mathrm{D}_{i,j,h}(Q_k;\mathrm{VS}) = \|\mathrm{VS} - Q_k\| + \|Q_k - h\| \tag{2}$$

where $\|\|$ represents the Euclidean distance and then, $\|\mathrm{VS} - Q_k\| = d_T$ is the transmit distance (from VS to the point Q_k), and $\|Q_k - h\| = d_R$ is the receive distance (from the point Q_k to the receive element h of transducer j). These distances are represented in Fig. 1.

Finally, the total beamformed image $S(Q_k;\mathrm{VS})$ can be obtained by coherently adding the individually beamformed images acquired in a sequence in which both probes transmit:

$$S(Q_k;\mathrm{VS}) = s_{1,1}(Q_k;\mathrm{VS}) + s_{1,2}(Q_k;\mathrm{VS}) + s_{2,1}(Q_k;\mathrm{VS}) + s_{2,2}(Q_k;\mathrm{VS}) \tag{3}$$

Note that, like in PW imaging, several waves at different angles (in this case defined by different VSs behind the probe) can be added to reconstruct a transmit focus [8].

Similar to CoMTUS with PW [2], the beamforming parameters that define Eq. 3, which include the average speed of sound in the propagation medium and the relative position and orientation of each imaging probe (defined by $\mathbf{r}_i$ and θ_i) are calculated by maximizing the similarity across RF datasets sharing the receive transducer for all common scatterers. Those parameters are the ones that define the total reception time corresponding to each scatterer and are:

$$\mathcal{P} = \{\mathrm{VS}, c, \theta_1, \mathbf{r}_1, \theta_2, \mathbf{r}_2, Q_1, \ldots, Q_K\} \tag{4}$$

In practice the position of the VS is known, and defining the world coordinate system the same as the local coordinate system of one of the transducers reduces the problem to $\mathcal{P} = \{c, \theta_2, \mathbf{r}_2, Q_1, \ldots, Q_K\}$.

The optimal parameters $\bar{\mathcal{P}}$ can be found maximizing the cost function χ by using gradient-based optimization methods [9] and initializing the algorithm in a similar way as in CoMTUS with PW [2],

$$\bar{\mathcal{P}} = \arg\max_{\mathcal{P}} \chi(\mathcal{P}) \tag{5}$$

Measuring the coherence by the normalized cross-correlation (NCC), the cost function quantifies the total coherence of the system over all receive transducers,

$$\chi(\mathcal{P}) = \sum_{k}^{K}\sum_{h}^{H}\{\mathrm{NCC}(T_1R_1(h,Q_k;\mathcal{P}), T_2R_1(h,Q_k;\mathcal{P}))W_{1,1}W_{2,1} + \mathrm{NCC}(T_1R_2(h,Q_k;\mathcal{P}), T_2R_2(h,Q_k;\mathcal{P}))W_{1,2}W_{2,2}\}$$

where $W_{i,j}$ is a weighting factor proportional to the degree of coherence between pulses received across the individual elements of a single transducer,

$$W_{i,j}(\mathcal{P}) = \frac{1}{2} + \frac{1}{2H}\sum_{h_b \neq h}^{H} \mathrm{NCC}(T_iR_j(h;\mathcal{P}), T_iR_j(h_b;\mathcal{P})) \tag{6}$$

III. Methods

The CoMTUS method using DWs was implemented in two synchronised 256-channel Ultrasound Advanced Open Platform (ULA-OP 256) systems (MSD Lab, University of Florence, Italy) [11], [12] to record images on an ultrasound phantom [2]. Each ULA-OP 256 system was connected to an ultrasonic linear array (imaging transducer LA332, Esaote, Firenze, Italy) made of 144 piezoelectric elements with a -6 dB bandwidth ranging from 2 MHz to 7.5 MHz. The probes were mounted on a multi-probe holder physical device to maintain them on the same imaging plane ($y = 0$) [13]. For each probe in an alternating sequence, DWs were generated by placing several VSs behind the probe and using the full array aperture as described in [14]. For non-steered DW, the VS was set behind the center of the probe with a distance equal to half aperture size to cover all elements with a DW opening angle of 60^o. For steered DW, multiple VSs were moving along a semi-circle (center: the center of the probe, radius: half aperture size) to different steering angles with respect to the vertical axis. The maximum steering angle was set as $\pm 15^o$. A total of 31 DWs were transmitted at 3 MHz and pulse repetition frequency (PRF) of 1 kHz linearly spaced to cover the total sector (-15^o to 15^o, 1^o step). RF raw data backscattered up to 85 mm deep were acquired at a sampling frequency of

19.5 MHz. Resulting CoMTUS images were compared with the equivalent images acquired by a single probe (T1). Image performance, in terms of spatial resolution and contrast, was assessed in all cases.

IV. Results

Fig. 2 shows a comparison between a DW image acquired with a single probe (T1) and the CoMTUS image. All images are shown in the same dynamic range of -45 dB. It is observed an overall improvement in the CoMTUS image. The speckle size is reduced and the different structures, point targets and anechoic region, are easily identifiable from the phantom background.

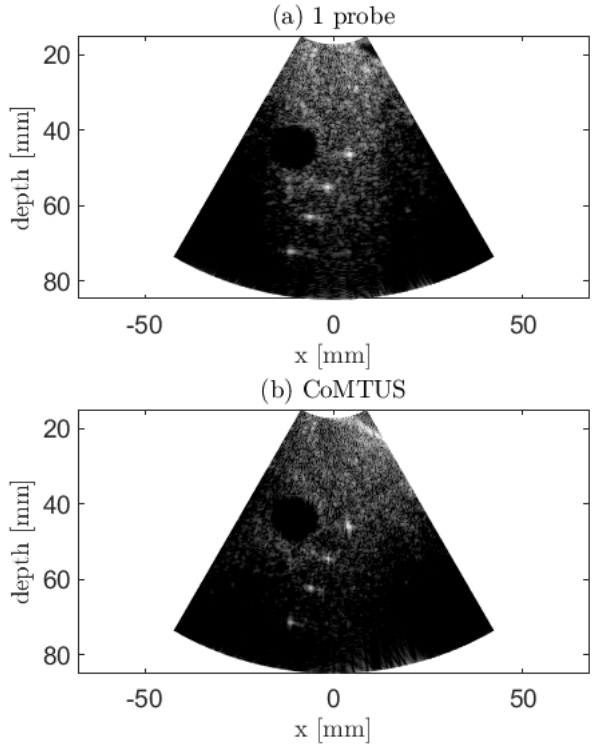

Fig. 2. Comparison of resulting images acquired by (a) a single probe; and (b) CoMTUS. Dynamic range -45 dB.

Lateral resolution was quantified from the point-spread function (PSF) of the four imaged point targets located at 46 mm, 55 mm, 62 mm and 71 mm depth, respectively. Contrast and contrast-to-noise ratio (CNR) were estimated at the anechoic lesion. The corresponding imaging metrics are summarized in Table I. Like in CoMTUS with PW [2], when using DWs the CoMTUS PSF has a significantly narrower main lobe but also side lobes of larger amplitude than a single probe conventional imaging system. For the DW single probe image, the measured lateral resolution at the different depths is 1.05 mm, 1.12 mm, 1.25 mm and 1.36 mm, while those values are reduced to 0.69 mm, 0.86 mm, 0.94 mm, and 1.06 mm, respectively, with an averaged improvement of 26 % in the CoMTUS image. In the single transducer case, the lesion is visible with a contrast of -19.79 dB and a CNR of 0.89, while both metrics are improved in the CoMTUS image to -22.06 dB and 0.92, respectively.

TABLE I
Imaging performance for the different methods

	Lateral Resolution [mm]				Contrast [dB]	CNR [-]
	46 mm depth	55 mm depth	62 mm depth	71 mm depth		
1 probe	1.05	1.12	1.25	1.36	-19.8	0.89
CoMTUS	0.69	0.86	0.94	1.06	-22.1	0.92

V. Discussion

This study shows the feasibility of increasing the effective aperture of the imaging system by the coherent combination of signals acquired by different synchronized transducers that have a shared FoV and transmit DWs. To estimate the required beamforming parameters, CoMTUS optimizes the spatial coherence of the backscattered echoes arising from the same point scatterer and received by the same transducer using sequential transmissions from each of the transducers.

Results show that the CoMTUS method, originally validated using PWs, can be adapted to DWs (see Fig. 2). Improvements in resolution, achieved with CoMTUS and DWs, agree with those achieved with PW, i.e. the lateral resolution is significantly smaller (-26%) when comparing with a single probe system of DW imaging. In addition, the resulting CoMTUS image has an enlarged FoV, expanding its possible applications. Although in Fig. 2 identical FoV is presented to aid comparison. Also, since the use of DWs expands the overlap of isonated regions, an improvement in the performance of the technique is expected.

However, the trade-off between resolution and contrast, previously observed in CoMTUS using PW, seems more critical with DWs. It is well known that the choice of the number and the position of VSs is crucial in the performance of all coherence compounding methods [6], [8] and thus will be also in CoMTUS. Further studies are needed to understand and determine the optimal transmit parameters in CoMTUS with DWs.

VI. Conclusions

This study extends CoMTUS imaging with DWs. The method was experimentally validated and improvements in imaging quality in terms of resolution and contrast have been shown. Results show that the CoMTUS method can be adapted to DWs. The use of DWs enlarges the imaging FoV, expanding the possible applications of CoMTUS.

Acknowledgment

This work was supported by the Wellcome Trust/EPSRC iFIND project, IEH Award [102431] (www.iFINDproject.com) and the Wellcome Trust/EPSRC funded Centre for Medical Engineering [WT 203148/Z/16/Z]. The authors acknowledge financial support from the Department of Health via the National Institute for Health Research (NIHR) comprehensive

Biomedical Research Centre award to Guy's & St Thomas' NHS Foundation Trust in partnership with King's College London and Kings College Hospital NHS Foundation Trust.

REFERENCES

[1] N. Bottenus, W. Long, H. K. Zhang, M. Jakovljevic, D. P. Bradway, E. M. Boctor, and G. E. Trahey, "Feasibility of swept synthetic aperture ultrasound imaging," IEEE Transactions on Medical Imaging, vol. 35, no. 7, pp. 1676–1685, 2016.

[2] L. Peralta, A. Gomez, Y. Luan, B. Kim, J.V. Hajnal, and R.J. Eckersley, "Coherent Multi-Transducer Ultrasound Imaging," IEEE Transactions on Ultrasonics, Ferroelectrics, and Frequency Control, vol. 66, no. 8, pp. 1316-1330, 2019.

[3] L. Peralta, A. Gomez, J.V. Hajnal, and R.J. Eckersley, "Feasibility study of a coherent multi-transducer US imaging system," In 2018 IEEE International Ultrasonics Symposium (IUS) (pp. 1-4). IEEE.

[4] L. Peralta, A. Gomez, J.V. Hajnal, and R.J. Eckersley, "Coherent multi-transducer ultrasound imaging in the presence of aberration," In Medical Imaging 2019: Ultrasonic Imaging and Tomography (Vol. 10955, p. 109550O). International Society for Optics and Photonics.

[5] G. Montaldo, M. Tanter, J. Bercoff, N. Benech, and M. Fink, "Coherent plane-wave compounding for very high frame rate ultrasonography and transient elastography," IEEE Transactions on Ultrasonics, Ferroelectrics and Frequency Control, vol. 56, no. 3, pp. 489–506, 3 2009.

[6] C. Papadacci, M. Pernot, M. Couade, M. Fink, and M. Tanter, "High-contrast ultrafast imaging of the heart," IEEE Transactions on Ultrasonics, Ferroelectrics, and Frequency Control, vol. 61, no. 2, pp. 288–301, 2014.

[7] A. W. Fitzgibbon, "Robust registration of 2d and 3d point sets, "Image and Vision Computing," vol. 21, no. 13-14, pp. 1145–1153, 2003.

[8] H. Hasegawa, and H. Kanai, "High-frame-rate echocardiography using diverging transmit beams and parallel receive beamforming," Journal of Medical Ultrasonics, vol. 38, no. 3, pp. 129–140, 2011.

[9] J. C. Lagarias, J. A. Reeds, M. H. Wright, and P. E. Wright, "Convergence properties of the Nelder-Mead simplex method in low dimensions," SIAM Journal on Optimization, vol. 9, no. 1, pp. 112–147, 1998.

[10] M. E. Anderson and G. E. Trahey, "The direct estimation of sound speed using pulse-echo ultrasound," The Journal of the Acoustical Society of America, vol. 104, no. 5, pp. 3099-3106, 1998.

[11] E. Boni, L. Bassi, A. Dallai, F. Guidi, V. Meacci, A. Ramalli, S. Ricci, and P. Tortoli, "Ula-op 256: A 256-channel open scanner for development and real-time implementation of new ultrasound methods," IEEE Transactions on Ultrasonics, Ferroelectrics and Frequency Control, vol. 63, no. 10, pp. 1488–1495, 2016.

[12] E. Boni, L. Bassi, A. Dallai, V. Meacci, A. Ramalli, M. Scaringella, F. Guidi, S. Ricci, and P. Tortoli, "Architecture of an ultrasound system for continuous real-time high frame rate imaging," IEEE Transactions on Ultrasonics, Ferroelectrics, and Frequency Control, vol. 64, no. 9, pp. 1276–1284, 2017.

[13] V. A. Zimmer, A. Gomez, Y. Noh, N. Toussaint, B. Khanal, R. Wright, L. Peralta, M. van Poppel, E. Skelton, J. Matthew, and J. A. Schnabel, "Multi-view image reconstruction: Application to fetal ultrasound compounding," in Melbourne A. et al. (eds) Data Driven Treatment Response Assessment and Preterm, Perinatal, and Paediatric Image Analysis. PIPPI 2018, DATRA 2018. Lecture Notes in Computer Science, vol 11076, pp. 107-116, 2018.

[14] F. Zhao, and J. Luo, "Diverging wave compounding with spatio-temporal encoding using orthogonal Golay pairs for high frame rate imaging," Ultrasonics, vol. 89, pp. 155–165, 2018.